Cancer Chemother Pharmacol (1999) 43: 507–515 © Springer-Verlag 1999

ORIGINAL ARTICLE

**Gregory P. Kalemkerian · Xiaolan Ou
Mohammed R. Adil · Rita Rosati · M. Monir Khoulani
Shashi K. Madan · George R. Pettit**

Activity of dolastatin 10 against small-cell lung cancer in vitro and in vivo: induction of apoptosis and bcl-2 modification

Received: 14 July 1998 / Accepted: 3 September 1998

Abstract *Purpose*: Dolastatin 10 is a natural cytotoxic peptide which acts through the inhibition of microtubule assembly. Studies have suggested that such agents can induce apoptosis in association with bcl-2 phosphorylation. Since *bcl-2* overexpression is common in small-cell lung cancer (SCLC), we evaluated the activity of dolastatin 10 in SCLC cell lines and xenografts. *Methods*: In vitro growth inhibition was evaluated with a standardized MTT assay and apoptosis with fluorescent microscopy and a TUNEL assay. Immunoblot analysis and phosphatase digestion were used to determine bcl-2 modification. In vivo activity was evaluated in subcutaneous and metastatic SCLC xenograft models in SCID mice. *Results*: Dolastatin 10 had growth inhibitory activity against four SCLC cell lines (NCI-H69, -H82, -H446, -H510) with IC_{50} values ranging from 0.032 to 0.184 n*M*. All four cell lines exhibited evidence of apoptosis after 48 h of exposure to 1.3 n*M* dolastatin 10. Immunoblot analysis revealed that 1.3 n*M* dolastatin 10 altered the electrophoretic mobility of bcl-2 in NCI-H69 and -H510 cells within 16 h of treatment. Incubation of protein extract from dolastatin 10-treated NCI-H69 and -H510 cells with calcineurin resulted in the disappearance of the altered mobility species, suggesting dolastatin 10-induced bcl-2 phosphorylation. In in vivo studies, 450 μg/kg of dolastatin 10 IV × 2 given after intravenous injection of NCI-H446 cells completely inhibited tumor formation. In established subcutaneous NCI-H446 xenografts, 450 μg/kg of dolastatin 10 IV induced apoptosis in the majority of tumor cells within 96 h, resulting in a $\log_{10}$ cell kill of 5.2 and an increase in median survival from 42 to 91 days. *Conclusions*: These findings suggest that dolastatin 10 has potent activity against SCLC and that the modulation of apoptotic pathways deserves further evaluation as an anticancer strategy.

Key words Dolastatin · Lung cancer · Apoptosis · Xenografts · Experimental therapeutics

Supported by the Charlotte A. Woody Lung Cancer Research Fund, the Harper Hospital Medical Staff Trust Fund, and the Webber Medical Advancement Fund (G.P.K.), and Outstanding Investigator Grant CA-44344-01A1-09, NCI, DHHS (G.R.P.).

G.P. Kalemkerian
Barbara Ann Karmanos Cancer Institute,
Wayne State University, Detroit, Michigan, USA

G.P. Kalemkerian (✉)
Division of Hematology and Oncology,
Harper Hospital, Hudson 5, 3990 John R,
Detroit, Michigan 48201, USA
e-mail: kalemker@karmanos.org
Tel.: +1-313-745-2357; Fax: +1313-993-0559

X. Ou
107 Roxboro Circle, #2, Syracuse, New York 13211, USA

M.R. Adil
28 Heritage Place, Glen Carbon, Illinois 62034, USA

R. Rosati
Barbara Ann Karmanos Cancer Institute,
110 E. Warren, Detroit, Michigan 48201, USA

M.M. Khoulani
10309 Queensbury Way, Fort Smith, Arkansas 72903, USA

S.K. Madan
Department of Pathology, Harper Hospital,
3990 John R, Detroit, Michigan 48201, USA

G.R. Pettit
Cancer Research Institute, Arizona State University,
P.O. Box 872404, Tempe, Arizona 85287-2404, USA

Introduction

Dolastatin 10, a unique peptide derived from the marine mollusk *Dolabella auricularia*, has been shown to have potent cytotoxic activity in preclinical models of human leukemia and lymphoma [3, 11, 16]. The mechanism of action of dolastatin 10 in hematopoietic cells appears to be the inhibition of microtubule assembly with subsequent mitotic arrest and apoptosis [2]. In addition, reports have suggested that dolastatin 10 exhibits cytotoxic activity in some preclinical solid tumor models [21, 22], but activity has not been evaluated in human

lung cancer. Phase I clinical trials of dolastatin 10 have been completed and phase II trials are underway.

The induction of apoptosis is an important mechanism of action of many cytotoxic agents and recent studies have suggested that the dysregulation of apoptotic pathways can play a significant role in the development of therapeutic resistance in cancer cells [7, 17]. The product of the *bcl-2* oncogene serves as an inhibitor of cell death in many, but perhaps not all, apoptotic pathways [19]. In vitro studies have demonstrated that bcl-2 expression inversely correlates with sensitivity to many chemotherapeutic agents [17] and that drug-induced bcl-2 phosphorylation is associated with the induction of apoptosis [5, 8, 9]. In small-cell lung cancer (SCLC), bcl-2 overexpression has been reported in most cell lines and primary tumors [4, 12, 20]. In addition, overexpression of exogenous *bcl-2* in one SCLC cell line inhibited apoptosis induced by some cytotoxic agents [15], and antisense bcl-2 oligonucleotides induced apoptosis in several SCLC cell lines [23], suggesting that bcl-2 overexpression may play a role in cell survival and treatment resistance in SCLC. The development of pharmacologic agents that modify bcl-2 expression and/or activity appears to be a rational strategy for novel anticancer therapy. We now report that dolastatin 10 has in vitro and in vivo cytotoxic activity against human SCLC cells, and that dolastatin 10-induced apoptosis in SCLC cells is associated with bcl-2 phosphorylation.

Materials and methods

Cell culture

Four small-cell carcinoma cell lines (NCI-H69, NCI-H82, NCI-H446 and NCI-H510) were obtained from ATCC (Rockville, Md.) and propagated in RPMI-1640 medium (Sigma, St. Louis, Mo.) supplemented with 5% fetal calf serum (Sigma), penicillin (100 μ/ml), streptomycin (100 μg/ml), and HITES (10 n*M* hydrocortisone, 15 μg/ml insulin, 100 μg/ml transferrin, 10 n*M* 17-β-estradiol, 30 n*M* selenium) in a humidified incubator at 37 °C under an atmosphere containing 5% CO_2. Dolastatin 10 was synthesized and supplied by G.R. Pettit.

Viability assay

Cells were treated with a range of concentrations of dolastatin 10 and seeded in 96-well plates with 200 μl/well and five wells per sample concentration at a density of $1–4 \times 10^4$ cells/ml. Control cells were treated with 0.1% DMSO and blank wells were loaded with medium only. After 5 days, 50 μl 1.0 mg/ml MTT (Sigma Chemicals, St. Louis, Mo.) was added to each well and the plates were incubated for 4 h at 37 °C prior to dissolution of formazan crystals in 200 μl DMSO. Absorbance at 570 nm (A_{570}) was determined for each well, and the survival fraction for each study condition was calculated from the ratio: (mean A_{570} treated cells – mean A_{570} blank wells)/(mean A_{570} control cells – mean A_{570} blank wells). The IC_{50} was determined with data from three experiments using CalcuSyn software (Biosoft, Cambridge, UK).

Flow cytometry

For DNA content analyses, 1×10^6 cells were exposed to either 0.1% DMSO or 1.3 n*M* dolastatin 10 for 24 or 48 h prior to fixation and staining with 5.0 μg/ml propidium iodide (PI) + RNase A. For the TUNEL (TdT-mediated dUTP nick-end labeling) assay, $2–4 \times 10^6$ cells were exposed to either 0.1% DMSO or 1.3 n*M* dolastatin 10 for up to 72 h prior to processing according to the ApopTag-Fluorescein (Oncor, Gaithersburg, Md.) protocol. Briefly, cells were incubated with TdT and digoxigenin-labeled dUTP followed by incubation with FITC-labeled anti-digoxigenin antibody (anti-dig-FITC) and counterstaining with 5 μg/ml PI. All samples were analyzed using a Becton-Dickinson (San Jose, Calif.) FACScan flow cytometer. Relative DNA content (PI) was detected with bandpass filter 585/42, and dUTP incorporation (anti-dig-FITC) with bandpass filter 530/30. For DNA histogram generation, the FACScan doublet discrimination circuit was employed. Data were analyzed using ModFit (Verity, Topsham, Me.) and/or PC-LYSYS software. All experiments were repeated at least twice.

Fluorescent microscopy

Cells ($1–3 \times 10^6$) were exposed to either 0.1% DMSO or 1.3 n*M* dolastatin 10 for up to 48 h prior to fixation and staining with 5.0 μg/ml PI + RNase A. All samples were analyzed on a Zeiss Laser Scanning Microscope LSM 310 with a 543 nm HENE laser. All experiments were repeated at least twice.

Immunoblot analysis

Cells were treated with either 0.1% DMSO or the indicated concentrations of dolastatin 10 prior to extraction of total cellular protein by sonication in lysis buffer (1 × PBS, 20 μg/ml aprotinin, 20 μg/ml leupeptin, 1.0 m*M* PMSF). Equivalent amounts of protein from each sample were separated via SDS-PAGE followed by electroblot transfer to Hybond C-Super membranes (Amersham, Arlington Heights, Ill.). For immunodetection, membranes were blocked prior to incubation with mouse monoclonal anti-bcl-2 or anti-β-actin primary antibody (Calbiochem, Cambridge, Mass.) at a 1:100 dilution for 1 h, followed by incubation with sheep anti-mouse Ig HRP-conjugated secondary antibody (Amersham) at a 1:1000 dilution for 1 h. Chemiluminescent detection was performed using ECL reagents (Amersham).

Phosphatase digestion

Total cellular protein (15 μg) extracted from cells treated with either 0.1% DMSO or 1.0 ng/ml (1.3 n*M*) dolastatin 10 for 24 h was incubated in reaction buffer (20 m*M* HEPES/KOH, pH 7.4, 5 m*M* $MgCl_2$, 1 m*M* $CaCl_2$, 0.5 U/μl calmodulin, 20 μg/ml aprotinin, 20 μg/ml leupeptin, 1.0 m*M* PMSF) with and without 1.0 U/μl calcineurin (Sigma Chemical Co.) for 30 min at 37 °C. Immunoblot analysis was then performed as described above.

In vivo studies

Inbred female CB-17 SCID mice (Taconic, Germantown, N.Y.) were obtained at 3 weeks of age. All experimental protocols were approved by the Wayne State University Animal Investigations Committee. All animals received cyclophosphamide 150 mg/kg × 1 subcutaneously in the dorsum of the neck 3 days prior to tumor cell inoculation. For subcutaneous (SC) xenograft experiments, animals were randomly divided into two experimental groups (control, $n = 8$; treated, $n = 10$) after injection of 5×10^6 cells in 0.1 ml PBS into each flank. Animals were evaluated at least every other day, and the tumor mass was estimated using the formula, tumor mass (mg) $= (a \times b^2)/2$, where a and b are tumor length and width, respectively. When the median tumor mass reached 100–150 mg (day 26), all animals in the treatment group received 450 μg/kg dolastatin 10 via the tail vein. Treatment was repeated on day 36. One control and two treated animals were sacrificed 48 and 96 h after the first dolastatin 10 injection and tumors were

harvested for histologic evaluation. The remaining six animals in each group were followed for tumor growth and survival.

Three methods were used to assess in vivo antitumor activity: (1) tumor growth delay, in terms of the T−C value, in which T is the median time (in days) required for the treatment group tumors to reach a predetermined size, and C is the median time (in days) for the control group tumors to reach the same size, using 2000 mg as the target tumor size; (2) tumor cell kill, in terms of $\log_{10}$ cell kill calculated using the formula, $\log_{10}$ kill (total) = (T−C)/($3.32 \times T_d$), in which T−C is the tumor growth delay (in days) as described above and T_d is the tumor volume doubling time (in days) estimated from control group tumors during exponential growth (500–1500 mg); and (3) tumor growth inhibition, calculated as $100 - (T/C \times 100)$, in which the median tumor mass in each group (C, control; T, treatment) was determined at a time when the control group's median tumor mass was between 750 and 1500 mg.

For IV xenograft experiments, all animals were randomly divided into two groups (control, $n = 8$; treatment, $n = 8$) after injection of 2×10^6 NCI-H446 cells in 0.1 ml PBS via the tail vein. Treatment group animals received 450 μg/kg dolastatin 10 on days 7 and 17 via the tail vein. Criteria for euthanasia included: tumor size ≥ 2000 mg, paralysis, inability to access food or water, weight loss >20%, respiratory distress, and central nervous system dysfunction.

Results

Inhibition of in vitro growth of SCLC cells by dolastatin 10

The cytotoxic activity of dolastatin 10 was evaluated in a heterogeneous panel of four human SCLC cell lines which represent the phenotypic, biochemical and genetic variability seen in SCLC tumors. Cell lines were exposed to a range of concentrations of dolastatin 10 for 5 days prior to the determination of viable cell survival via a standardized MTT assay. A dose-response relationship was noted in all cell lines, with IC_{50} values of 0.032–0.184 n*M* and IC_{95} values of 0.49–2.7 n*M* (Table 1). Exposure of NCI-H82 cells to 0.16–1.3 n*M* of dolastatin 10 for 8 h prior to washout resulted in 80–96% of the cytotoxicity seen in cells exposed to dolastatin 10 continuously for 96 h (data not shown).

Induction of apoptosis in SCLC cells in vitro by dolastatin 10

SCLC cells were exposed to 1.3 n*M* dolastatin 10 for 24 and 48 h prior to flow cytometric DNA content analysis. All four cell lines exhibited a substantial increase in the percentage of cells arrested in the G_2/M phase of the cell cycle (Table 2, Fig. 1A). In addition, the percentage of cells containing a subdiploid DNA content was increased after exposure to 1.3 n*M* dolastatin 10 for 48 h (NCI-H69, 19.9% vs 1.3%; NCI-H82, 43.3% vs 5.5%; NCI-H446, 57.3% vs 4.0%; NCI-H510, 25.3% vs 4.0%), suggesting an increase in apoptotic cells with nucleosomal DNA fragmentation. A quantitative TUNEL assay demonstrated that the percentage of NCI-H69 and NCI-H446 cells with increased dUTP incorporation, consistent with apoptosis, rose substantially after 48 h treatment with 1.3 n*M* dolastatin 10 (Fig. 1B). A similar increase in the percentage of apoptotic cells was observed in similarly treated NCI-H82 and NCI-H510 cells (data not shown). Fluorescent microscopic evaluation of PI-stained SCLC cells revealed typical apoptotic features in NCI-H69, NCI-H82, NCI-H446 and NCI-H510 cells after exposure to 1.3 n*M* dolastatin 10 for 48 h (Fig. 2). These features included cellular shrinkage, cytoplasmic vacuolization, chromatin condensation and nuclear fragmentation into apoptotic bodies. These findings suggest that dolastatin 10 inhibits growth through a rapid induction of apoptotic pathways in SCLC cell lines.

Table 1 Growth inhibitory effect of dolastatin 10. Values are the means of at least three experiments

Cell line	IC_{50} ± SE (n*M*)
NCI-H82	0.032 ± 0.008
NCI-H446	0.048 ± 0.011
NCI-H69	0.059 ± 0.003
NCI-H510	0.184 ± 0.005

Table 2 Cell cycle analysis after exposure to dolastatin 10 for 24 h. Values are the means of at least three experiments ± SD (*D10* 1.3 n*M* of dolastatin 10)

	G_0/G_1 (%)	S (%)	G_2/M (%)
NCI-H69	48.1 ± 4.9	34.4 ± 3.6	17.5 ± 1.3
NCI-H69 + D10	9.9 ± 3.1	16.1 ± 6.3	74.0 ± 9.0
NCI-H82	43.5 ± 2.6	34.7 ± 3.0	21.8 ± 3.3
NCI-H82 + D10	17.1 ± 1.7	28.0 ± 4.1	54.9 ± 5.8
NCI-H446	54.8 ± 6.5	38.3 ± 3.7	7.0 ± 3.3
NCI-N446 + D10	7.4 ± 4.3	10.0 ± 4.5	52.7 ± 5.0
NCI-H510	45.9 ± 3.4	45.5 ± 2.0	8.5 ± 1.2
NCI-H510 + D10	8.3 ± 4.3	33.6 ± 5.4	58.2 ± 9.6

Bcl-2 modification in SCLC cells after dolastatin 10 treatment

NCI-H69 and NCI-H510 cells express relatively high levels of bcl-2, while NCI-H446 and NCI-H82 cells express very low levels of bcl-2. Immunoblot analysis revealed a dose-dependent alteration in the bcl-2 electrophoretic pattern in NCI-H69 and NCI-H510 cells exposed to at least 1.0 ng/ml (1.3 n*M*) of dolastatin 10 for 24 h (Fig. 3A). This altered pattern consisted of the appearance of one to two bands with slightly slower mobility, suggesting post-translational modification. Faint alterations in bcl-2 expression were detectable in NCI-H446 cells, while bcl-2 could not be detected in NCI-H82 cells. In NCI-H69 cells, the species with slower mobility were evident by 16 h and overall expression of bcl-2 decreased after 48 h of exposure to 1.3 n*M* dolastatin 10 (Fig. 3B). To determine whether this modification represented bcl-2 phosphorylation, total cellular protein from NCI-H69 and NCI-H510 cells exposed to 1.3 n*M* of dolastatin 10 for 24 h was incubated with calcineurin, a calcium-calmodulin-dependent type 2B

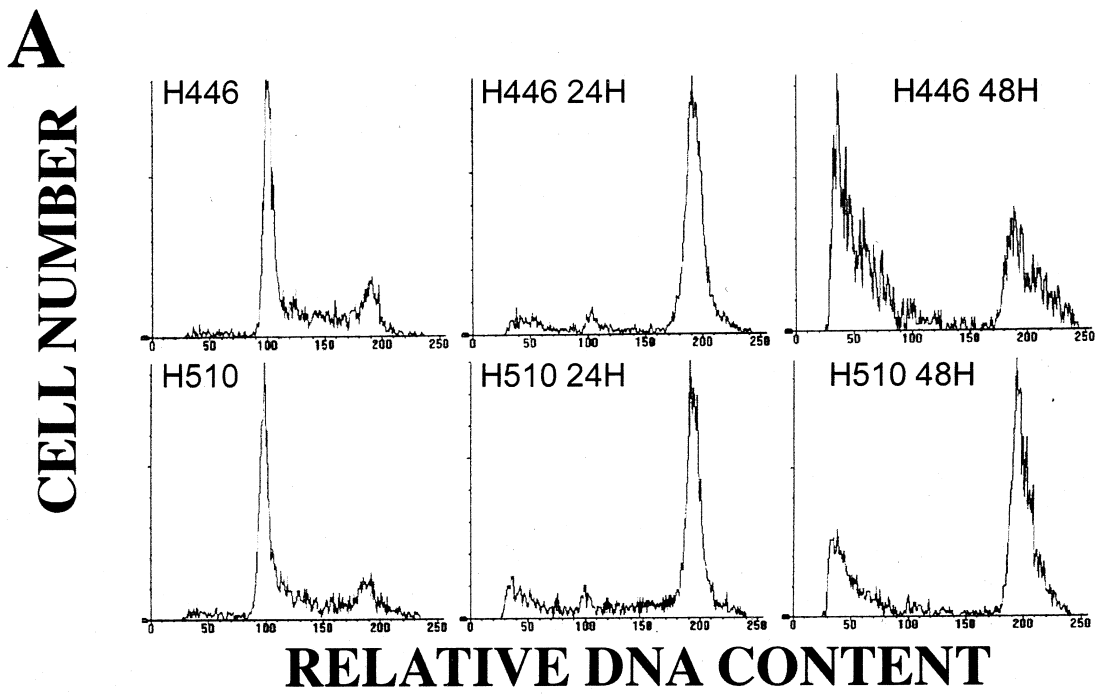
A
CELL NUMBER
H446
H446 24H
H446 48H
H510
H510 24H
H510 48H
RELATIVE DNA CONTENT

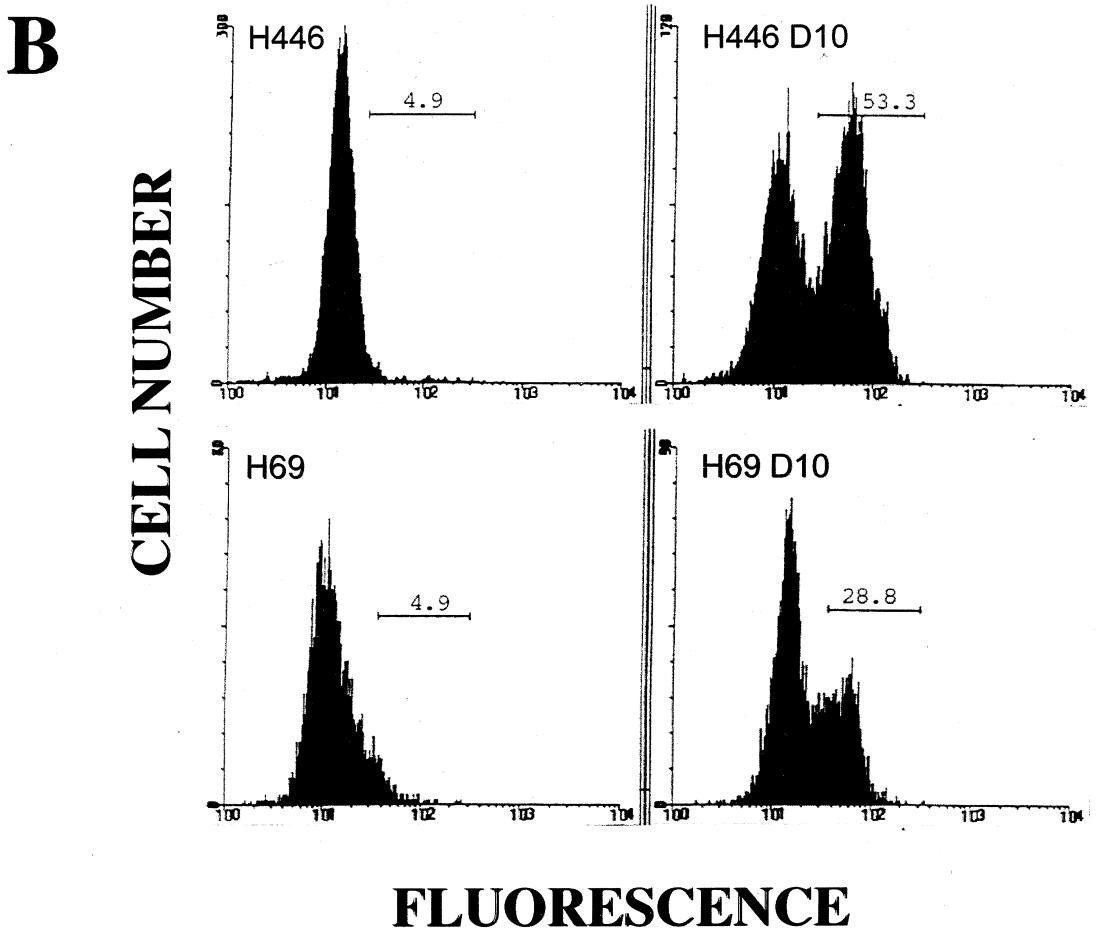
B
CELL NUMBER
H446
4.9
H446 D10
53.3
H69
4.9
H69 D10
28.8
FLUORESCENCE

◀

Fig. 1 **A** DNA content analysis: NCI-H446 (*top row*) and NCI-H510 (*bottom row*) exposed to 0.1% DMSO (*left*) or 1.3 n*M* dolastatin 10 for 24 h (*center*) or 48 h (*right*). Note G_2/M arrest at 24 h and emergence of subdiploid peak at 48 h. **B** TUNEL assay: single-parameter histograms of $\log_{10}$ FITC fluorescence indicating digoxigenin-UTP (d-UTP) incorporation by anti-digoxigenin-FITC antibody labeling. Percentages indicate cells with increased d-UTP incorporation, correlating with apoptosis, as determined by integration of the area under the curve within fixed marker limits (range 40–400). NCI-H446 and NCI-H69 cells were exposed to either 0.1% DMSO (*left*) or 1.3 n*M* of dolastatin 10 (*right*) for 48 h

phosphatase, in the presence of protease inhibitors to prevent nonspecific proteolysis. Calcineurin treatment resulted in restoration of the original $p26^{bcl-2}$ band and disappearance of the species with slower mobility (Fig. 3C), supporting the hypothesis that dolastatin 10 induces bcl-2 phosphorylation. Similar results have been observed in NCI-H69 and NCI-H510 cells after treatment with paclitaxel (data not shown).

In vivo activity of dolastatin 10 in SCLC xenografts

We have developed two efficient xenograft models using the NCI-H446 SCLC cell line in CB-17 SCID mice. In the first model, intravenous injection of 2×10^6 cells via the tail vein results in widespread disease in all animals in an anatomic pattern resembling metastatic human SCLC. In the second model, subcutaneous bilateral flank injection of 5×10^6 cells results in palpable tumors in over 90% of injection sites within 3 weeks of tumor cell injection, but no evidence of metastatic disease.

Table 3 summarizes the activity of dolastatin 10 in the metastatic SCLC xenograft model. This experiment demonstrated that intravenous injection of 450 μg/kg dolastatin 10 on days 7 and 17 after intravenous tumor cell injection completely inhibited the formation of NCI-H446 xenografts in all eight treated animals. These animals all remained healthy, except for transient weight loss following drug administration, until they were eu-

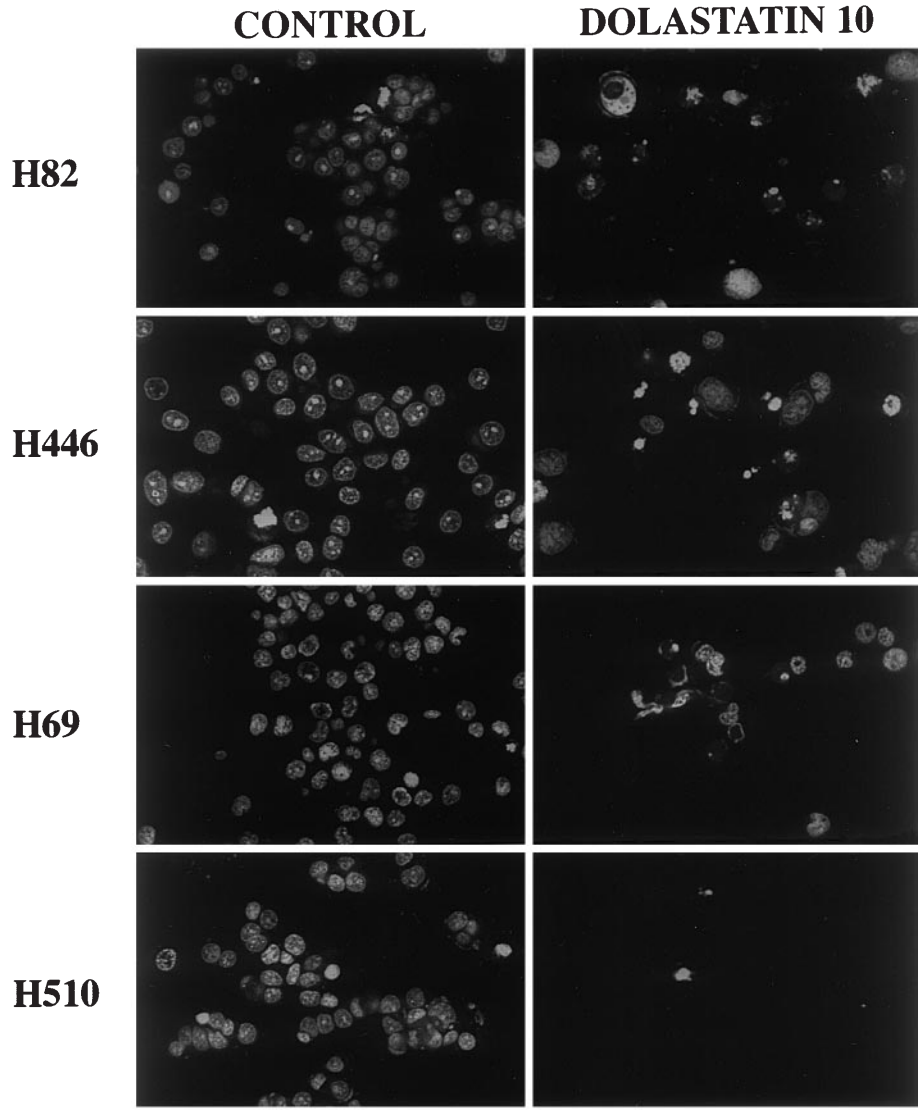

Fig. 2 Fluorescent micrographs of SCLC cells exposed to 0.1% DMSO (*control*) or 1.3 n*M* of dolastatin 10 (*dolastatin 10*) for 48 h. Note cellular shrinkage, chromatin condensation and nuclear fragmentation consistent with apoptosis in all cell lines following exposure to dolastatin 10 (×600)

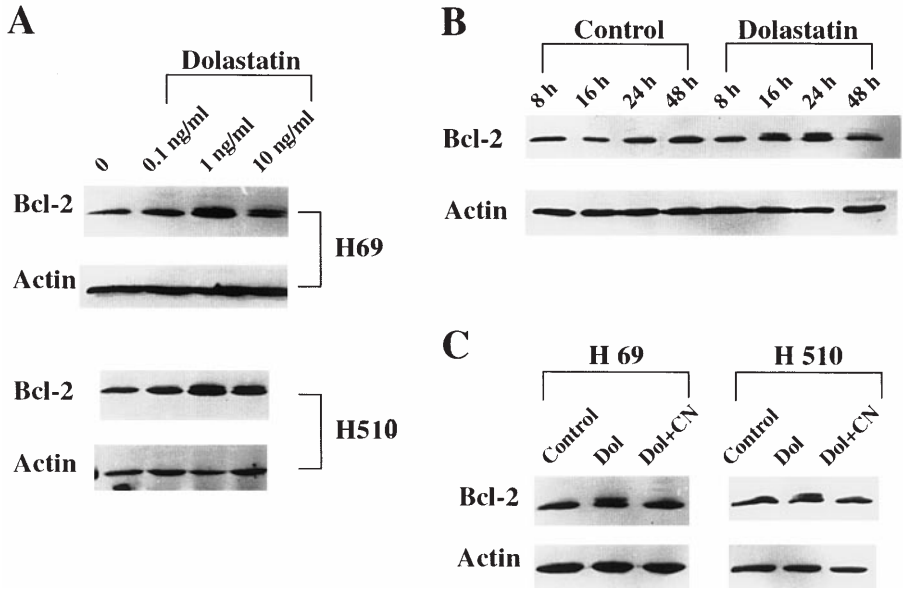

Fig. 3 **A** Immunoblot analysis with 15 μg total cellular protein from the noted SCLC cell lines exposed to either 0.1% DMSO (*lane 1*) or increasing concentrations of dolastatin 10 (*lanes 2–4*) for 24 h. Membranes were sequentially probed with monoclonal bcl-2 and β-actin antibodies followed by chemiluminescent immunodetection. Note the emergence of species with slower mobility in NCI-H69 and NCI-H510 cells in a dose-dependent manner. β-actin denotes equivalence of loading. **B** Immunoblot analysis with 15 μg total cellular protein from NCI-H69 cells treated with either 0.1% DMSO (*control, lanes 1–4*) or 1.0 ng/ml (1.3 n*M*) dolastatin 10 (*lanes 5–8*) for the noted times. The membrane was sequentially probed with monoclonal bcl-2 and β-actin antibodies. β-actin denotes equivalence of loading. **C** Immunoblot analysis of phosphatase assay with 15 μg total cellular protein from NCI-H69 or NCI-H510 cells exposed to either 0.1% DMSO (*Control, lanes 1 and 4*) or 1.0 ng/ml (1.3 n*M*) dolastatin 10 for 24 h without (*Dol*, *lanes 2 and 5*) or with (*Dol+CN*, *lanes 3 and 6*) in vitro incubation of protein extract with calcineurin. Note disappearance of species with slower mobility after incubation with calcineurin. β-actin denotes equivalence of loading

Table 3 Inhibition of intravenous NCI-H446 xenografts with dolastatin 10

	Control (n = 8)	Dolastatin 10 (n = 8)
Dose	–	450 μg/kg IV × 2
Schedule	–	Days 7 and 17
Mean weight change (%)		
Day 9 vs day 7	−6.1	−9
Day 19 vs day 17	+1.1	−6.3
Tumor latency (days)		
Median	54.5	–
Range	44–63	–
Survival (days)		
Median	59	214[a]
Range	53–72	–

[a] All animals euthanized with no evidence of disease

thanized on day 214 at which time thorough necropsies revealed no gross or microscopic evidence of disease. In contrast, all eight control animals developed clinical evidence of metastatic tumors by day 63 and were euthanized with progressive disease at multiple sites by day 72 after tumor cell injection (Table 3).

In order to determine the in vivo activity of dolastatin 10 against established SCLC tumors, subcutaneous xenografts were allowed to reach a median mass of 100–150 mg before animals were treated intravenously with 450 μg/kg dolastatin 10 on days 26 and 36 (Table 4). Dolastatin 10 induced measurable shrinkage in all tumors and had a profound effect on tumor growth inhibition, tumor growth delay, $\log_{10}$ cell kill and survival when compared to control animals (Table 4). One dolastatin 10-treated animal had no gross or microscopic evidence of disease after euthanasia on day 107 after tumor cell injection. To evaluate the in vivo induction of apoptosis, additional control and treated animals were sacrificed 48 and 96 h following the first dose of dolastatin 10 and tumors were removed for histopathologic evaluation. By 48 h apoptotic cells were evident in all tumors from treated animals and by 96 h the majority of cells appeared to be apoptotic (Fig. 4).

Discussion

In the present study, dolastatin 10 exhibited potent growth inhibitory activity against a panel of genetically heterogeneous SCLC cell lines with apoptosis observed within 48 h of exposure to 1.3 n*M* dolastatin 10. In addition, dolastatin 10 had profound effects on the growth of metastatic and subcutaneous SCLC xenografts in SCID mice. The reported mechanism of action of dolastatin 10 involves the interruption of tubulin polymerization with subsequent mitotic arrest and cell death. An additional aspect of this mechanism is suggested, but not proven, by the finding that dolastatin 10-induced apoptosis was associated with bcl-2 phosphorylation in SCLC cells that inherently overexpress bcl-2. Phase I clinical studies have shown that transient peak

Table 4 Treatment of established subcutaneous NCI-H446 xenografts with dolastatin 10

	Control (n = 6)	Dolastatin 10 (n = 6)
Dose	–	450 μg/kg IV
Schedule	–	Days 26 and 36
Mean body weight change (%)		
Day 30 vs day 26	+1.3	−16.3
Day 38 vs day 36	−1.2	−6.1
Tumor mass on day 26 (mg)		
Median	116	122
Range	6–320	48–221
Tumor mass on day 40 (mg)		
Median	1635	44
Range	1080–2176	6–113
Tumor growth inhibition (100 − (T/C × 100))	–	97
Tumor growth delay (T−C days)[a]	–	50
Log_{10} cell kill	–	5.2
Survival (days)		
Median	42	91
Range	40–42	71–107
Tumor-free on day 107	0/6	1/6

[a] Excludes one animal cured of tumor

Fig. 4A–D Photomicrographs of NCI-H446 subcutaneous xenografts after H&E staining: **A** control (×1000), **B** 48 h after treatment with dolastatin 10 (×1000), **C** 96 h after treatment with dolastatin 10 (×1000), **D** 96 h after treatment with dolastatin 10 (×2500). Note cellular shrinkage, nuclear condensation and nuclear fragmentation after dolastatin 10 treatment

serum concentrations of 100 nM are achievable after a single dose of dolastatin 10, with a subsequent plateau of 1.0–2.0 nM and a serum half-life of 8–20 hours [1, 18]. These phase I studies have also demonstrated that myelosuppression is the dose-limiting toxicity of dolastatin

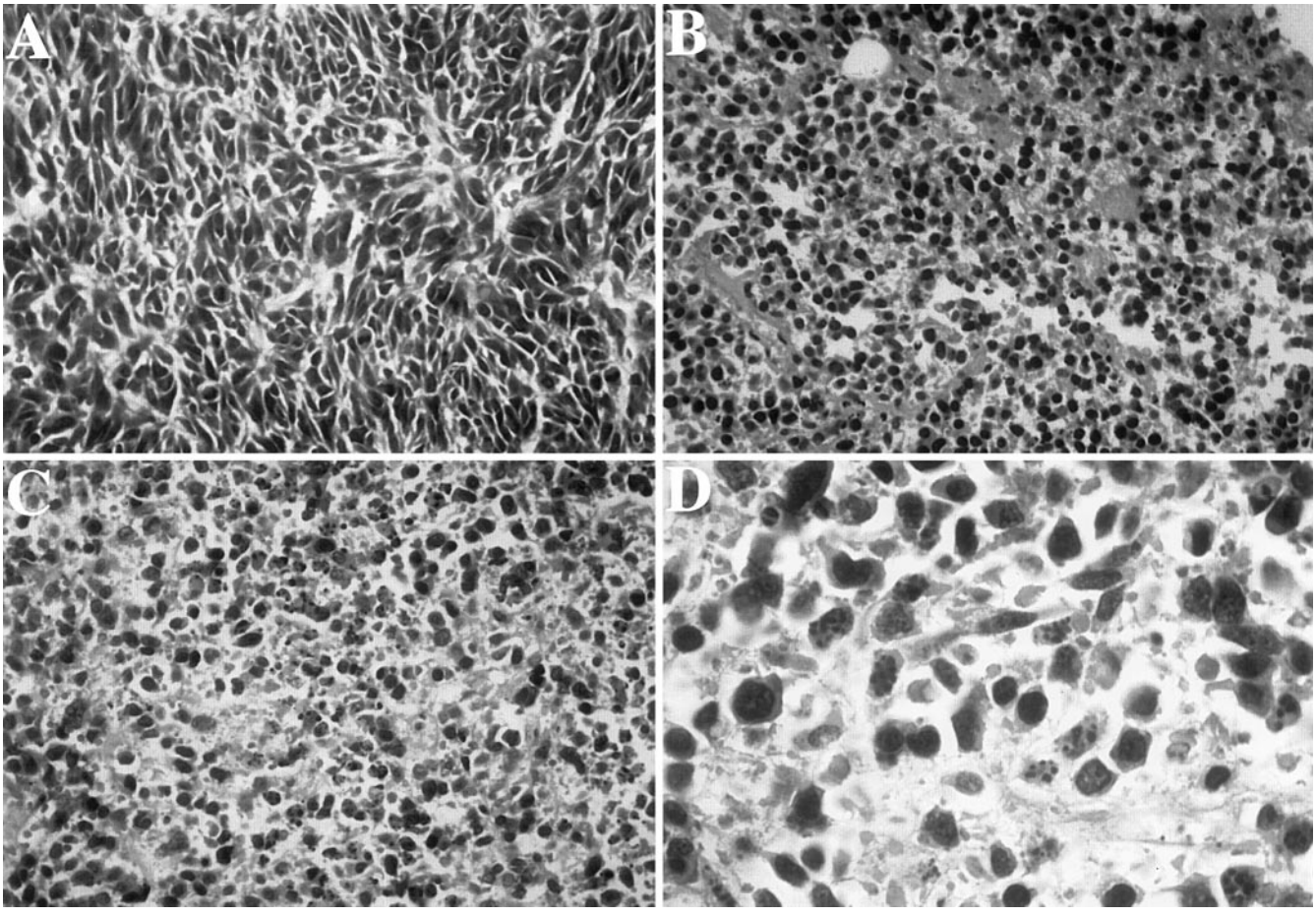

10. Although dolastatin 10 induced substantial weight loss in our in vivo studies, it did not affect the animals' activity level nor result in other observable toxicity. Overall, these findings suggest that clinical studies to evaluate dolastatin 10 in patients with lung cancer are justified.

Despite a high rate of response to initial therapy, nearly all patients with SCLC relapse and die with treatment-resistant disease, resulting in a 5-year survival of less than 10%. The molecular events involved in the progression of SCLC are poorly understood and the role of novel molecular mechanisms of treatment resistance, such as *bcl-2* overexpression, remains unknown. Evidence suggests that alterations in the activity of bcl-2 and related proteins can greatly affect the efficacy of radiation and chemotherapy in a variety of malignant cell types, including SCLC [15, 17]. For example, antisense inhibition of bcl-2 expression has been shown to increase sensitivity to cytotoxic agents in both hematopoietic and SCLC cells [13, 23]. Clinical reports have suggested that the overexpression of bcl-2 is associated with poor response to therapy and/or poor overall survival [17]. Therefore, the lowering of the apoptotic threshold in cancer cells via the inactivation of bcl-2 function may be a rational therapeutic strategy.

Although drug-induced bcl-2 phosphorylation has been associated with apoptosis in several malignant cell types, a causal relationship between the modification of bcl-2 and the induction of cell death has yet to be demonstrated. Thus far, several cytotoxic agents that induce G_2/M arrest through interactions with tubulin, but not those acting through other mechanisms, have been reported to induce bcl-2 phosphorylation in association with apoptosis [6, 10]. In contrast, May et al. [14] have reported that bcl-2 phosphorylation, albeit without a molecular weight shift on immunoblot analysis, leads to a suppression of apoptosis following growth factor withdrawal in murine myeloid cells, suggesting increased bcl-2 activity after phosphorylation. The disparate effects of bcl-2 phosphorylation on apoptosis may be explained by variations in the expression of other apoptotic mediators in different cell types or the effects of phosphorylating agents on other components of the apoptotic pathways. We have noted that dolastatin 10 has no effect on bax expression and are further characterizing apoptotic mediators in SCLC cells.

Although our findings suggest that dolastatin 10-induced apoptosis is associated with bcl-2 phosphorylation in SCLC cells, it remains possible that the observed alteration in bcl-2 does not reflect phosphorylation or that apoptosis in this setting is independent of any bcl-2 modification. However, since many cytotoxic agents exert their cytotoxic effects through bcl-2-dependent apoptotic pathways, compounds such as dolastatin 10 that post-translationally modify bcl-2, may be useful additions to future anticancer regimens.

Acknowledgements We are grateful to Dr. Mary L. Varterasian for critical review of the manuscript; Dr. Patricia LoRusso, Ms. Chiab Panchapor and Dr. Ramzi Mohammad for assistance with in vivo studies; and Ms. Linda Mayernik for production of the figures. We also thank the Analytical Cytometry and Confocal Imaging Core Facilities (supported in part by center grants NCI-P30CA22453 and NIEHS-P30ES06639).

References

1. Bagniewski PG, Reid JM, Pitot HC, Sloan JA, Ames MM (1997) Pharmacokinetics of dolastatin 10 in adult patients with solid tumors. Proc Am Assoc Cancer Res 38: 221
2. Bai R, Pettit GR, Hamel E (1990) Binding of dolastatin 10 to tubulin at a distinct site for peptide antimitotic agents. J Biol Chem 28: 17141
3. Beckwith M, Urba WJ, Longo DL (1993) Growth inhibition of human lymphoma cell lines by the marine products, dolastatins 10 and 15. J Natl Cancer Inst 85: 483
4. Ben-Ezra JM, Kornstein MJ, Grimes MM, Krystal G (1994) Small cell carcinomas of the lung express the bcl-2 protein. Am J Pathol 145: 1036
5. Blagosklonny MV, Schulte T, Nguyen P, Trepel J, Neckers LM (1996) Taxol-induced apoptosis and phosphorylation of bcl-2 protein involves c-raf-1 and represents a novel c-raf-1 signal transduction pathway. Cancer Res 56: 1851
6. Blagosklonny MV, Giannakakou P, El-Deiry WS, Kingston DGI, Higgs PI, Neckers L, Fojo T (1997) Raf-1/bcl-2 phosphorylation: a step from microtubule damage to cell death. Cancer Res 57: 130
7. Fisher DE (1995) Apoptosis in cancer therapy: crossing the threshold. Cell 78: 539
8. Haldar S, Jena N, Croce CM (1995) Inactivation of bcl-2 by phosphorylation. Proc Natl Acad Sci USA 92: 4507
9. Haldar S, Chintapalli J, Croce C (1996) Taxol induces bcl-2 phosphorylation and death of prostate cancer cells. Cancer Res 56: 1253
10. Haldar S, Basu A, Croce C (1997) Bcl-2 is the guardian of microtubule integrity. Cancer Res 57: 229
11. Hu ZB, Gignac SM, Quentmeier H, Pettit GR, Drexler HG (1993) Effects of dolastatins on human B-lymphocytic leukemia cell lines. Leuk Res 17: 333
12. Ikegaki N, Katsumata M, Minna J, Tsujimoto Y (1994) Expression of bcl-2 in small cell lung carcinoma cells. Cancer Res 54: 6
13. Keith FJ, Bradbury DA, Zhu YM, Russell NH (1995) Inhibition of bcl-2 with antisense oligonucleotides induces apoptosis and increases the sensitivity of AML to Ara-C. Leukemia 9: 131
14. May WS, Tyler G, Ito T, Armstrong DK, Qatsha KA, Davidson NE (1994) Interleukin-3 and bryostatin-1 mediate hyperphosphorylation of BCL2α in association with suppression of apoptosis. J Biol Chem 269: 26865
15. Ohmori T, Podack ER, Nishio K, Takahashi M, Miyahara Y, Takeda Y, Kubota N, Funayama Y, Ogasawara H, Ohira T, Ohta S, Saijo N (1993) Apoptosis of lung cancer cells caused by some anti-cancer agents is inhibited by bcl-2. Biochem Biophys Res Commun 192: 30
16. Pettit GR, Kamano Y, Herald CL, Tuinman AA, Boetner FE, Kizu H, Schmidt JM, Baczynskyj L, Tomer KB, Bontems RJ (1987) The isolation and structure of a remarkable marine animal antineoplastic constituent: dolastatin 10. J Am Chem Soc 109: 6883
17. Reed JC (1995) Bcl-2: prevention of apoptosis as a mechanism of drug resistance. Hematol Oncol Clin North Am 9: 451
18. Tran HT, Newman RA, Beck DE, Huie R, Abbruzzese JL, Madden T (1997) A phase I, pharmacokinetic/pharmacodynamic study of dolastatin-10 in adult patients with advanced solid tumors. Proc Am Assoc Cancer Res 38: 306
19. Vaux DL, Cory S, Adams JM (1988) Bcl-2 gene promotes hematopoietic cell survival and cooperates with c-myc to immortalize pre-B cells. Nature 335: 440
20. Walker C, Robertson L, Myskow M, Dixon G (1995) Expression of the bcl-2 protein in normal and dysplastic

bronchial epithelium and in lung carcinomas. Br J Cancer 72: 164
21. Waud WR, Dykes DJ, Pettit GR, Plowman J (1993) Preclinical antitumor activity of dolastatin 10. Proc Am Assoc Cancer Res 34: 383
22. Winterhalter BR, Berger DP, Pettit GR, Fiebig HH (1991) Cytotoxicity of dolastatin 10, dolastatin 15 and dolastatin K333 in human tumor xenografts in vitro. Proc Am Assoc Cancer Res 32: 402
23. Ziegler A, Luedke GH, Fabbro D, Altmann KH, Stahel RA, Zangemeister-Wittke U (1997) Induction of apoptosis in small-cell lung cancer by an antisense oligonucleotide targeting the bcl-2 coding sequence. J Natl Cancer Inst 89: 1027